Biochimica et Biophysica Acta 1838 (2014) 1088–1095

Contents lists available at ScienceDirect

Biochimica et Biophysica Acta

journal homepage: www.elsevier.com/locate/bbamem

The ORF4a protein of human coronavirus 229E functions as a viroporin that regulates viral production ☆

Ronghua Zhang [a,b,1], Kai Wang [b,1], Wei Lv [b,1], Wenjing Yu [b], Shiqi Xie [b], Ke Xu [b], Wolfgang Schwarz [c,d], Sidong Xiong [a,*], Bing Sun [b,e,**]

[a] Jiangsu Key Laboratory of Infection and Immunity, Institutes of Biology and Medical Sciences, Soochow University, Suzhou 215123, China
[b] Key Laboratory of Molecular Virology and Immunology, Institut Pasteur of Shanghai, Shanghai Institutes for Biological Sciences, Chinese Academy of Sciences, Shanghai 200025, China
[c] Goethe-University Frankfurt, Institute for Biophysics, Max-von-Laue-Str. 1, D-60438 Frankfurt am Main, Germany
[d] Shanghai Research Center for Acupuncture and Meridian, 199 Guoshoujing Road, Shanghai 201023, China
[e] State Key Laboratory of Cell Biology, Institute of Biochemistry and Cell Biology, Shanghai Institutes for Biological Sciences, Chinese Academy of Sciences, Shanghai 200031, China

ARTICLE INFO

Article history:
Received 19 March 2013
Received in revised form 12 July 2013
Accepted 18 July 2013
Available online 29 July 2013

Keywords:
HCoV-229E
ORF4a
Homo-oligomers
Ion channel
Viroporin

ABSTRACT

In addition to a set of canonical genes, coronaviruses encode additional accessory proteins. A locus located between the spike and envelope genes is conserved in all coronaviruses and contains a complete or truncated open reading frame (ORF). Previously, we demonstrated that this locus, which contains the gene for accessory protein 3a from severe acute respiratory syndrome coronavirus (SARS-CoV), encodes a protein that forms ion channels and regulates virus release. In the current study, we explored whether the ORF4a protein of HCoV-229E has similar functions. Our findings revealed that the ORF4a proteins were expressed in infected cells and localized at the endoplasmic reticulum/Golgi intermediate compartment (ERGIC). The ORF4a proteins formed homo-oligomers through disulfide bridges and possessed ion channel activity in both *Xenopus* oocytes and yeast. Based on the measurement of conductance to different monovalent cations, the ORF4a was suggested to form a non-selective channel for monovalent cations, although Li^+ partially reduced the inward current. Furthermore, viral production decreased when the ORF4a protein expression was suppressed by siRNA in infected cells. Collectively, this evidence indicates that the HCoV-229E ORF4a protein is functionally analogous to the SARS-CoV 3a protein, which also acts as a viroporin that regulates virus production. This article is part of a Special Issue entitled: Viral Membrane Proteins — Channels for Cellular Networking.

© 2013 Elsevier B.V. All rights reserved.

1. Introduction

Coronaviruses (CoVs) are positive-stranded, enveloped RNA viruses belonging to the family *Coronaviridae*, order *Nidovirales*. CoVs are widely distributed among vertebrates and cause respiratory, enteric or neurologic disease [1]. Historically, only five human CoVs (HCoVs) were recognized, including HCoV-229E [2], HCoV-OC43 [3], SARS-CoV [4–6], HCoV-NL63 [7] and HCoV-HKU1 [8]. However, a novel human CoV was recently isolated from a patient in Saudi Arabia with acute pneumonia and renal failure and was proposed to be a novel species in the genus *Betacoronavirus* [9,10].

The HCoV genome is 27–32 Kb in size and consists of a set of canonical genes: 5′-capped–replicase–spike (S)–envelop (E)–membrane (M)–nucleocapsid (N)–3′-polyadenylated [1]. In addition, some species-specific accessory open reading frames (ORFs) are interspersed among the structural genes. A locus located between S and E is conserved in all CoV genomes [11], and its encoding protein has been studied in several different CoVs. Studies have shown that the SARS-CoV 3a protein has ion channel activity [12], regulates virus production [13] and induces host cell apoptosis [14]. In HCoV-NL63, the ORF3 protein was shown to be N-glycosylated and to function as a structural viral protein [15]. Similar to HCoVs, porcine epidemic diarrhea virus (PEDV) and transmissible gastroenteritis virus (TGEV) ORF3 proteins were shown to be involved in viral pathogenicity [16–18]. These results suggest the importance of this accessory protein for the life cycle of CoVs. HCoV-229E encodes ORF4a, a truncated accessory protein at this locus, but its function is still unknown.

Abbreviations: CoV, coronavirus; HCoV, human coronavirus; SARS-CoV, severe acute respiratory syndrome coronavirus; ORF, open reading frame; PEDV, porcine epidemic diarrhea virus; TGEV, transmissible gastroenteritis virus; ERGIC, endoplasmic reticulum/Golgi intermediate compartment; β-ME, β-mercaptoethanol; TMD, transmembrane domain; cRNA, complementary RNA; ORi, oocyte Ringer's-like solution; TEVC, two-electrode voltage clamp; MOI, multiplicity of infection; $TCID_{50}$, 50% tissue culture infective dose

☆ This article is part of a Special Issue entitled: Viral Membrane Proteins — Channels for Cellular Networking.

* Corresponding author. Tel./fax: +86 512 65881255.
** Correspondence to: B. Sun, Key Laboratory of Molecular Virology and Immunology, Institut Pasteur of Shanghai, Shanghai Institutes for Biological Sciences, Chinese Academy of Sciences, 225 South Chongqing Road, Shanghai 200025, China. Tel.: +86 21 63851927; fax: +86 21 63843571.
E-mail addresses: sdxiongfd@126.com (S. Xiong), bsun@sibs.ac.cn (B. Sun).

[1] Authors who contributed equally to this work.

0005-2736/$ – see front matter © 2013 Elsevier B.V. All rights reserved.
http://dx.doi.org/10.1016/j.bbamem.2013.07.025

In this study, we investigated the expression, molecular properties and functions of the HCoV-229E ORF4a protein and found that it may be a new viroporin. The ORF4a protein formed disulfide-linked homo-oligomers and was predicted to possess three transmembrane domains (TMDs), which indicate that ORF4a could function as an ion channel. The putative ion channel activity of ORF4a was proven in *Xenopus* oocytes and yeast by the two-electrode voltage clamp (TEVC) and the yeast potassium uptake complementation assay, respectively. Furthermore, the production of HCoV-229E was reduced in infected human hepatocellular carcinoma (Huh-7) cells when ORF4a expression was blocked by siRNA. In conclusion, our study supports that the HCoV-229E protein may function as a viroporin to regulate virus production. This finding will be helpful for understanding HCoV-229E pathogenesis, and it suggests a novel target for developing drugs against HCoV-229E.

2. Materials and methods

2.1. Cell culture, transfection and virus infection

HEK293T and Huh-7 cells were cultured in Dulbecco's modified Eagle's medium (DMEM; Thermo Fisher Scientific, Beijing, China) supplemented with 10% fetal bovine serum (FBS; Gibco, Grand Island, NY, USA), penicillin (100 U/ml) and streptomycin (100 μg/ml) at 37 °C in a humidified atmosphere with 5% CO_2. 293T and Huh-7 cells were transfected with plasmids using Lipofectamine 2000 reagent (Invitrogen, Grand Island, NY, USA), following the manufacturer's instructions. Huh-7 cells were inoculated with HCoV-229E (VR-740) (ATCC, Manassas, VA, USA) at a multiplicity of infection (MOI) of 0.1 for 1 h in medium without serum. Cells were then washed with phosphate-buffered saline (PBS) and cultured with DMEM supplemented with 2% FBS at 37 °C for 2–5 d.

2.2. Plasmids

Total RNA from the HCoV-229E infected cells were extracted using Trizol reagent (Invitrogen, Carlsbad, CA, USA) following manufacturer's instruction. cDNA was synthesized by the ReverTra Ace qPCR RT kit (Toyobo, Osaka, Japan). The ORF4a coding sequence with HA or Flag tag at the C-terminus was cloned into the pCAGGS vector (a kind gift from Jun-ichi Miyazaki, Osaka University) for expression. The HCoV-229E ORF4a-HA sequence was subcloned into the pNWP vector (a kind gift from Jian Fei, Shanghai Institute of Biological Science) for cRNA in vitro transcription. The ORF4a-HA sequence was also subcloned into a yeast expression vector pYES2 (a kind gift from Wei Song, Shanghai Institute of Biological Science) for the yeast potassium uptake complementation assay. The pYES2 vector contains a URA3 gene as a selectable marker for positive transformants in *ura*-negative hosts. The exogenous gene is controlled by the *GAL1* promoter, and its expression was induced in the presence of galactose. All plasmids were verified by direct sequencing.

2.3. Antibodies

The polyclonal antibody anti-ORF4a was obtained from the Antibody Research Center (Shanghai Institute of Biochemistry and Cellular Biology, Chinese Academy of Sciences). The anti-HA monoclonal antibody (MMS-101P) was purchased from Covance (Berkeley, CA, USA), and the anti-Flag monoclonal antibody (F3165) was purchased from Sigma-Aldrich (St. Louis, MO, USA). Anti-HA (H6908) and anti-Flag (F7425) polyclonal antibodies were both purchased from Sigma-Aldrich (St. Louis, MO, USA). For immunofluorescence analysis, the ERGIC53 antibody (B-9), a murine monoclonal antibody against the endoplasmic reticulum/Golgi intermediate compartment (ERGIC), was utilized (Santa Cruz Biotechnology, Santa Cruz, CA, USA).

2.4. Immunoprecipitation and Western blot

For immunoprecipitation, transfected 293T cells were lysed in RIPA buffer with protease inhibitor. Cell lysates were centrifuged at 15,000 ×*g* for 20 min at 4 °C, and the supernatant was incubated with EZview Red anti-Flag M2 affinity gel (F2426, Sigma-Aldrich, St. Louis, MO, USA) at 4 °C overnight. The gels were then washed 5 times with RIPA buffer and lysed in SDS loading buffer for further analysis. The lysates were separated by 12% SDS-PAGE and transferred to nitrocellulose membranes (Bio-Rad, Hercules, CA, USA). The immunoblot analysis was performed as described previously [12].

2.5. Immunofluorescence and confocal microscopy

Huh-7 cells were transiently transfected with the ORF4a-HA expression plasmid on pretreated glass slides in 24-well plate. Twenty-four hours after transfection, cells were washed with PBS, fixed with 4% paraformaldehyde (PFA) and then permeabilized with 0.3% Triton X-100. The cells were blocked and immunolabeled with polyclonal anti-HA and monoclonal anti-ERGIC53 antibodies, followed by a Cy3-conjugated goat anti-rabbit antibody (111-165-045, Jackson, West Grove, PA, USA) and an Alexa Fluor 488-conjugated goat anti-mouse antibody (A11029, Molecular Probes, Invitrogen, Carlsbad, CA, USA). Localization of the ORF4a protein was examined using a TCS SP2 confocal microscope (Leica Microsystems, Wetzlar, Germany).

2.6. Electrophysiological measurements

HCoV-229E ORF4a-HA cRNA was synthesized from the pNWP-ORF4a-HA vector using the mMESSAGE mMACHINE high-yield capped RNA transcription SP6 kit (Ambion, Austin, TX, USA). For current recording, *Xenopus laevis* oocytes were obtained and maintained as described previously [12]. Healthy oocytes in stage V to VI were injected with 20–25 ng of cRNA. Injected oocytes were incubated at 18 °C in an ND-96 solution (96 mM NaCl, 2 mM KCl, 1.8 mM $CaCl_2$, 1 mM $MgCl_2$, 2.5 mM pyruvate and 5 mM HEPES, adjusted to pH 7.4 with NaOH) and were used for electrophysiology analysis 36–48 h after cRNA injection. A two-electrode voltage clamp (OC-725C, Warner Instruments, Hamden, CT, USA) was used to record the currents from the plasma membranes of *Xenopus* oocytes. The standard voltage-clamp protocol consisted of rectangular voltage steps from −150 to +30 mV in 10-mV increments applied from a holding voltage of −60 mV. The microelectrodes were filled with 3 M KCl and had a resistance of 1–2 MΩ. During the current recording, the oocytes were bathed in the ORi solution (90 mM NaCl, 2 mM KCl, 2 mM $CaCl_2$ and 5 mM HEPES, pH = 7.4 with NaOH) at room temperature (approximately 22 °C). For the ion substitution assay, a bath solution containing 92 mM XCl (LiCl, NaCl, KCl, RbCl or CsCl), 2 mM $CaCl_2$ and 5 mM HEPES, adjusted to pH 7.4 with Tris base, was used. Current recording and analysis were performed with pClamp 10.0 software (Molecular Devices, Sunnyvale, CA, USA).

2.7. Yeast potassium uptake complementation assay

Either the empty pYES2 or the pYES2-ORF4a-HA vector was transformed into a potassium uptake-deficient yeast strain W303 R5421 (*ura*3-52 *his*3Δ200 *leu*2Δ1 *trp*1Δ1 *ade*2 *trk1*Δ::HIS3 trk2Δ::HIS3) (a kind gift from Richard F. Gaber, Northwestern University) using the lithium acetate procedure. Yeast potassium uptake complementation experiments were performed as previously described [18,19]. Briefly, transformants were selected on yeast nitrogen-based (YNB) media without uracil, supplemented with the required amino acid and 100 mM KCl. Yeast cells from the same stock were diluted and grown in parallel on media without uracil, supplemented with 100 mM or 0.2 mM KCl. Plates were kept at 30 °C during the growth experiments.

2.8. HCoV-229E ORF4a siRNA knockdown

siRNAs targeting HCoV-229E ORF4a were designed as previously described [18] and chemically synthesized by the Genepharma Company (Shanghai, China). The siORF4a sequence was the following: sense 5′-UUUCUCAACUAAACUUCCUdTdT-3′, and antisense 5′-AGGAAGUUUA GUUGAGAAAdTdT-3′. Huh-7 cells were transfected with 100 pmol siRNA using the X-tremeGENE siRNA transfection reagent (Roche, Mannheim, Germany). After incubation for 24 h, cells were infected with HCoV-229E at an MOI of 0.1. Forty-eight hours after infection, the amount of extracellular infectious virus was measured by $TCID_{50}$ assay.

3. Results

3.1. Comparison of HCoV-229E ORF4a amino acid sequence with SARS-CoV 3a

CoVs were classified into four genera by The International Committee on Taxonomy of Viruses (ICTV). The HCoV-229E and SARS-CoV are belonging to the genera *Alphacoronavirus* and *Betacoronavirus*, respectively [20]. The ORF4a of HCoV-229E is only 133 amino acids in size, while it occurs with 274 amino acids to the homologous SARS-CoV 3a protein. The amino acid sequence alignment revealed that ORF4a and 3a share about 17% identity, though 3a has a much longer protein sequence (Fig. 1A). Application of transmembrane domain (TMD) prediction programs revealed that the ORF4a protein was predicted to possess three TMDs with an extracellular N-terminus and an intracellular C-terminus: TM1 (Val-40 to Leu-59), TM1 (Leu-71 to Ser-89) and TM3 (Ala-95 to Leu-115) (Fig. 1B). This predicted membrane topology of ORF4a is similar to SARS-CoV 3a protein, except for a truncated cytoplasmic peptide [12,21]. In spite of a low degree of protein sequence identity, HCoV-229E ORF4a has the general structure similar to SARS-CoV 3a.

3.2. Identification of the ORF4a protein in HCoV-229E-infected cells

To identify the expression of ORF4a in HCoV-229E (VR-740, ATCC) in infected Huh-7 cells, a rabbit polyclonal antiserum against a peptide derived from the predicted ORF4a protein was used in a Western blot assay. A specific band with a corresponding molecular weight (approximately 17 kDa) can be observed in the HCoV-229E-infected Huh-7 cell lysates but not in the lysates from mock-infected cells (Fig. 2A). Next, we attempted to determine the intracellular localization of the ORF4a protein. The expression plasmid containing the HCoV-229E ORF4a sequence with an HA tag at the C-terminus was constructed and transfected into the Huh-7 cells. As shown in Fig. 2B, the ORF4a protein co-localized with the ERGIC. This is consistent with the localization of the homologous HCoV-NL63 ORF3 [15] and SARS-CoV 3a proteins [22,23]. The similarity of structural topology and localization between ORF4a and 3a suggests that the two proteins possess similar properties or functions.

3.3. The ORF4a protein forms homo-oligomers through covalent disulfide bonds

Because the SARS-CoV 3a protein could form cysteine-linked homodimers and homotetramers [12], we suspected that the HCoV-229E ORF4a protein might also form homo-oligomers. To address this question, we first performed a coimmunoprecipitation assay. The ORF4a-HA protein coimmunoprecipitated with the ORF4a-Flag protein (Fig. 3A), suggesting that the ORF4a proteins form homo-oligomers. Next, to assess whether disulfide bonds are involved in the ORF4a protein polymerization, we treated or untreated the immunoprecipates with β-mercaptoethanol (β-ME), which reduces disulfide bonds within proteins, before running SDS-PAGE gels. As shown in Fig. 3B, when the immunoprecipates were not treated with β-ME, the monomers (17 kDa) and putative dimers (34 kDa), trimers (51 kDa), tetramers (68 kDa) and pentamers (85 kDa) were detected by immunoblot analysis using an anti-Flag antibody. However, the oligomer bands

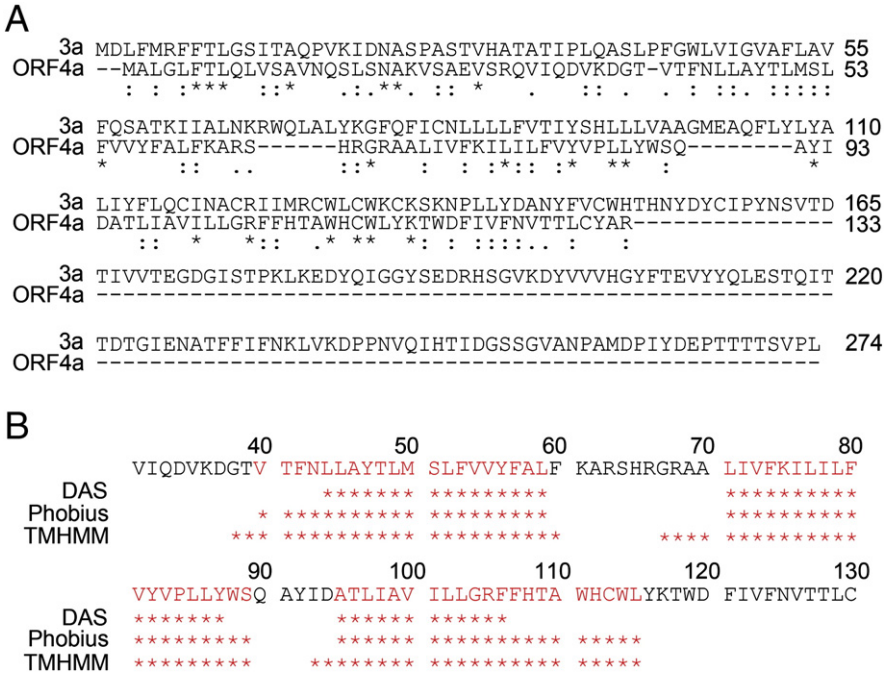

Fig. 1. Sequence alignment and structure prediction of HCoV-229E ORF4a. (A) Amino acid sequence alignment of HCoV-229E ORF4a with SARS-CoV 3a using ClustalW2. The "*" indicates identical residues, the ":" indicates conserved substitution and the "." indicates semi-conserved substitution. (B) Prediction of the transmembrane (TM) domains of the ORF4a protein. Three different programs were used to predict the TMs of ORF4a, including DAS, Phobius and TMHMM. The red letters indicate the putative TMs.

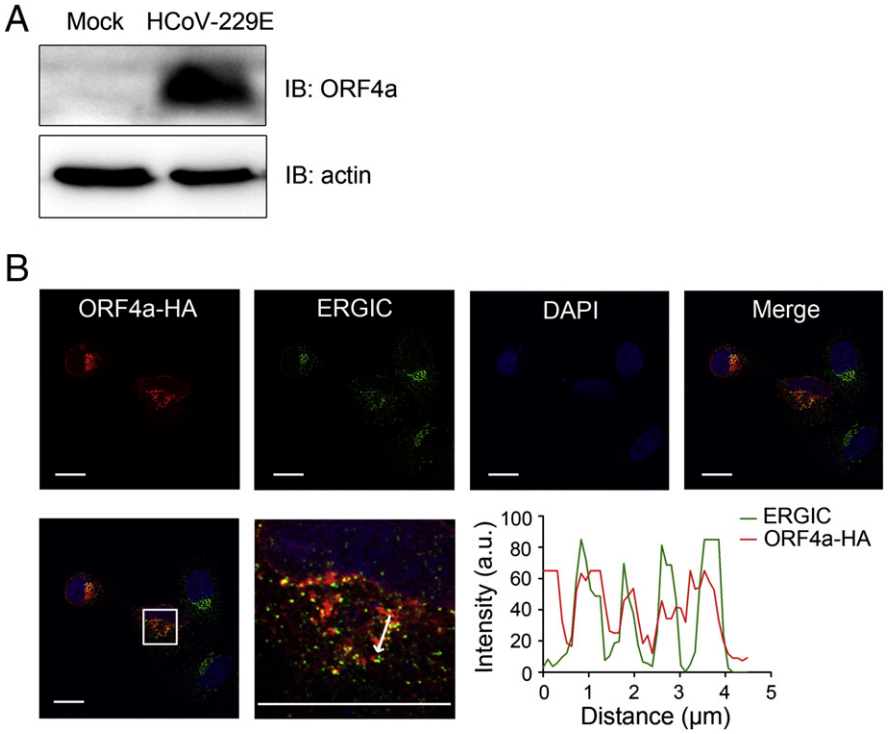

Fig. 2. The expression and subcellular localization of the HCoV-229E ORF4a protein. (A) The ORF4a protein was detected in HCoV-299E-infected Huh-7 cells using Western blot analysis. Huh-7 cells were infected with HCoV-229E at an MOI of 0.1 or mock-infected as a control. (B) Subcellular localization of the ORF4a protein in transfected Huh-7 cells. The ORF4a protein was detected with rabbit anti-HA antibody and visualized with Cy3-conjugated goat anti-rabbit antibody (red). ERGIC was detected with mouse anti-ERGIC-53 antibody (B-9) and visualized with Alexa Fluor 488-conjugated goat anti-mouse antibody (green). The nuclei were counterstained with DAPI (blue). Yellow signals in merged pictures show colocalization. White box and arrow correspond to colocalization analysis of fluorescence intensities (arbitrary units) of the dyes that were measured by ImageJ software, and shown next to the image. Bars represent 25 μm.

were abolished after treatment with β-ME, suggesting that disulfide bridges were necessary for ORF4a oligomer formation.

3.4. The ORF4a protein serves as ion channels in Xenopus oocytes and yeast

In our previous study, we demonstrated that the SARS-CoV 3a and PEDV ORF3 proteins induce membrane current on *Xenopus* oocytes [12,18]. As described above, the ORF4a protein might be a transmembrane protein and form homo-oligomers in the membrane, which pointed to ion channel formation as a potential function for this protein. To assess the putative ion channel activity of ORF4a, healthy *Xenopus* oocytes were injected with C-terminally HA-tagged ORF4a complementary RNA (cRNA), and oocyte membrane currents were recorded using a two-electrode voltage clamp. All procedures followed those described previously [24]. Macroscopic currents were recorded in the ORF4a-HA cRNA-injected oocytes and were compared to uninjected oocytes (control oocytes) of the same batch (Fig. 4A). Fig. 4B displays the current–voltage (*I/V*) relationship recorded from oocytes expressing ORF4a protein and control oocytes. Intriguingly, the channel conductance was approximately linear from −100 to +30 mV but exhibited an enhanced slope from −150 to −100 mV (Fig. 4B). These results revealed that the ORF4a protein could enhance oocyte membrane permeability and generate an instantaneous current that was voltage-dependent.

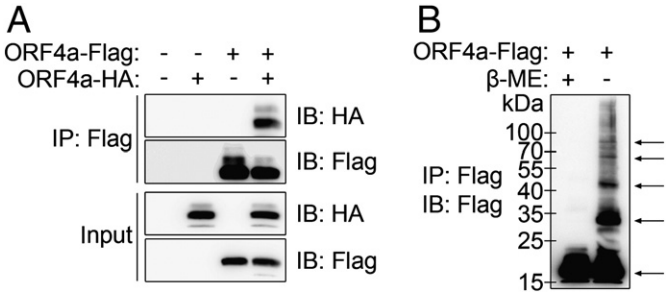

Fig. 3. The ORF4a protein forms homo-oligomers. (A) HEK293T cells were transfected with pCAGGS-ORF4a-HA or pCAGGS-ORF4a-Flag plasmids and subjected to immunoprecipitation with a monoclonal anti-Flag antibody. The associated HA-tagged ORF4a protein was detected using Western blot analysis with a polyclonal anti-HA antibody. (B) The HEK293 cells were transfected with pCAGGS-ORF4a-Flag. Cell lysates were immunoprecipitated with anti-Flag antibody and treated or not treated with β-mercaptoethanol (β-ME). The ORF4a proteins were detected by immunoblot analysis using the anti-Flag antibody. The arrows indicate bands corresponding to the monomer and putative oligomers.

To further characterize the ion channel activity of ORF4a, we performed a yeast potassium uptake complementation assay with a potassium uptake-deficient strain of *Saccharomyces cerevisiae*, which grow poorly on low-potassium medium. As shown in Fig. 4C, the growth of mutant yeast in the low-potassium (0.2 mM) medium could be rescued when expressing the ORF4a protein, whereas yeast transformed with an empty vector only grew well on high-potassium (100 mM) medium. These results indicated that the ORF4a protein could also form ion channels in the yeast plasma membrane and increase its permeability to K^+ ions. Therefore, the HCoV-229E ORF4a protein forms ion channels in *Xenopus* oocytes and yeast membrane.

3.5. Selectivity of ORF4a ion channel to different monovalent cations

Because the ORF4a channel is permeable to K^+ in yeast, we next assessed whether ORF4a could transport other cations. By performing two electrode voltage clamp experiments, we evaluated the selectivity of ORF4a ion channels to different monovalent cations. Ion substitution

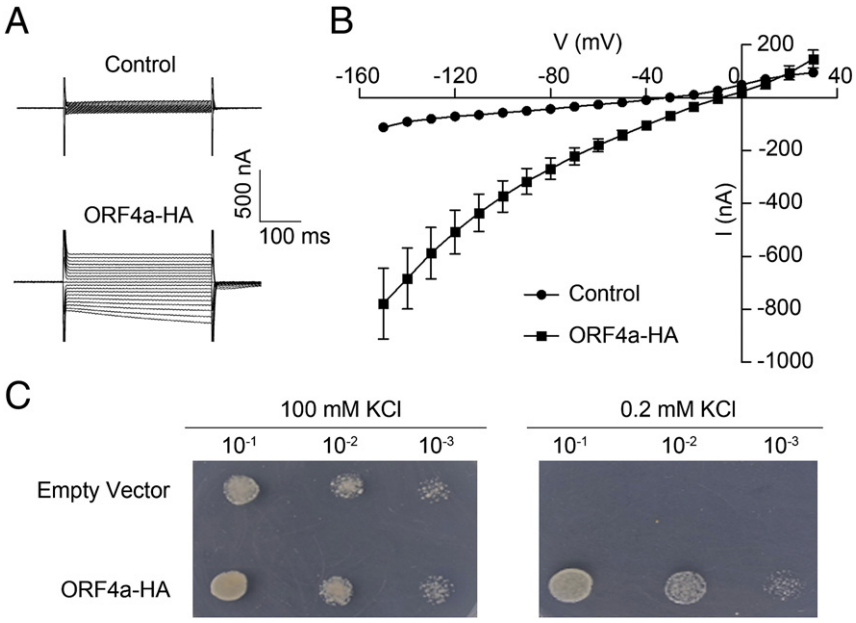

Fig. 4. The ORF4a protein forms ion channels in *Xenopus* oocytes and yeast. (A) Representative current traces were recorded by two-electrode voltage clamp (TEVC) step from −150 to +30 mV in non-injected control oocytes and ORF4a-HA-expressing oocytes of the same batch. (B) The *I/V* relationship of voltage dependencies of steady-state currents in control oocytes (filled circles) and ORF4a-HA-expressing oocytes (filled squares). Current values were averaged across all oocyte batches tested. Data represent the mean ± SEM. (C) Complementation of a potassium uptake-deficient strain of *S. cerevisiae* with a pYES2-ORF4a-HA or pYES2 empty vector. The transformed yeast was grown on media containing 100 mM KCl or 0.2 mM KCl. Yeast was diluted as indicated and inoculated on the plates.

revealed that replacing the external monovalent cations with Na^+, K^+, Rb^+ or Cs^+ had no statistically significant effect on inward current amplitude, but the Li^+ partially reduced the inward current in all oocyte batches tested (Fig. 5A and B). At positive voltages there was an indication of outward current only for K^+ and Rb^+, suggesting Li^+, Na^+ and Cs^+ exhibited some inhibitory effect on outward current in this positive potential range (Fig. 5A). Since the constant field theory is invalid to estimate the permeability of many ion channels [25], we focused to calculate the ion selectivity of ORF4a to monovalent cations from the ratios of slope conductances at negative potentials. As shown in Fig. 5C, the relative conductances of ORF4a to the monovalent cations were not significantly different. Thus, ORF4a protein may form a non-selective channel for monovalent cations.

3.6. The suppression of ORF4a expression in virus-infected cells results in decreasing HCoV-229E production

A growing family of viral proteins, named viroporins, is significant in the viral life cycle and has attracted increasing attention from researchers [26–31]. Viroporins share common characteristics: they are small proteins with 50–120 amino acids and contain at least one hydrophobic transmembrane domain that oligomerizes in the membrane to form hydrophilic pores. These pores permeabilize membranes by transporting ions or small molecules, and these activities participate in many steps of the viral life cycle, such as the entry, assembly and release of viral particles [12,32–34]. As described above, the ORF4a protein possesses the features of viroporins, suggesting that the HCoV-229E ORF4a protein could be a new member of the viroporin family. To confirm this, the correlation between ORF4a expression and virus production was tested. A siRNA specifically targeted to the HCoV-229E ORF4a gene was designed (siORF4a), and its knockdown efficiency was determined using Western blot analysis (Fig. 6A). The viral infectious particles in the supernatant were titered by $TCID_{50}$ assay. As shown in Fig. 6B, the amount of extracellular infectious virus was significantly reduced when 100 pmol siORF4a was used. These results suggested that the ORF4a protein acts as a viroporin and is necessary for HCoV-229E propagation.

4. Discussion

Previously, we showed that the SARS 3a protein forms a viral ion channel and regulates virus production. Although the protein sequence alignment showed a little sequence homology between HCoV-229E ORF4a and SARS 3a protein, our data suggest that their functional characteristics are nearly the same. In this study, we confirmed that the ORF4a protein is a new member of the viroporins that contains the common features of this family, such as oligomerization, enhancement of membrane permeability and regulation of virus production. Using the polyclonal antibody anti-ORF4a, we demonstrated that the ORF4a protein could be expressed in HCoV-229E-infected cells. We also analyzed the localization of the ORF4a protein and determined that it was localized to the ERGIC, which is the assembling and budding site of CoVs [1], suggesting that the ORF4a protein might participate in the assembly or release process during HCoV-229E infection. Additionally, we found that the ORF4a protein self-oligomerized, which is an outstanding feature of ion channels [26]. Based on this result, we assumed that the ORF4a protein could form an ion channel. To confirm this, we tested the ion channel activity in both *Xenopus* oocytes and yeast cells. Indeed, ORF4a expressed in *Xenopus* oocytes or yeast could conduct ions and enhance membrane permeability. Most viroporins were structured by disulfide bonds or noncovalent interactions to form a tetrameric or pentameric channel [35,36]. The ORF4a protein has only two cysteines at its C-terminus, suggesting that the ORF4a protein is linked by protein–protein disulfide bonds to form a homo-pentamer channel structure. The exact number of monomers and the ion channel structure still need to be investigated.

Because ORF4a could form ion channels at the yeast cell membrane and render it permeable to K^+, we tested the ion selectivity of the ORF4a protein to the monovalent cations. According to the conductance ratios, ORF4a protein may form a non-selective channel to the monovalent cations. Other viroporins, such as the HIV-1 Vpu and the HCV p7, also have been reported to form cation-selective channels and show equal selectivity for Na^+ and K^+ [37,38]. Mehnert et al. have studied the selectivity of Vpu TM peptide to different monovalent cations in vitro using artificial lipid membrane and show a conductance increase in the series $Li^+ < Na^+ < K^+ < Rb^+ < Cs^+$ [39]. Another viroporin, Kcv, encoded by

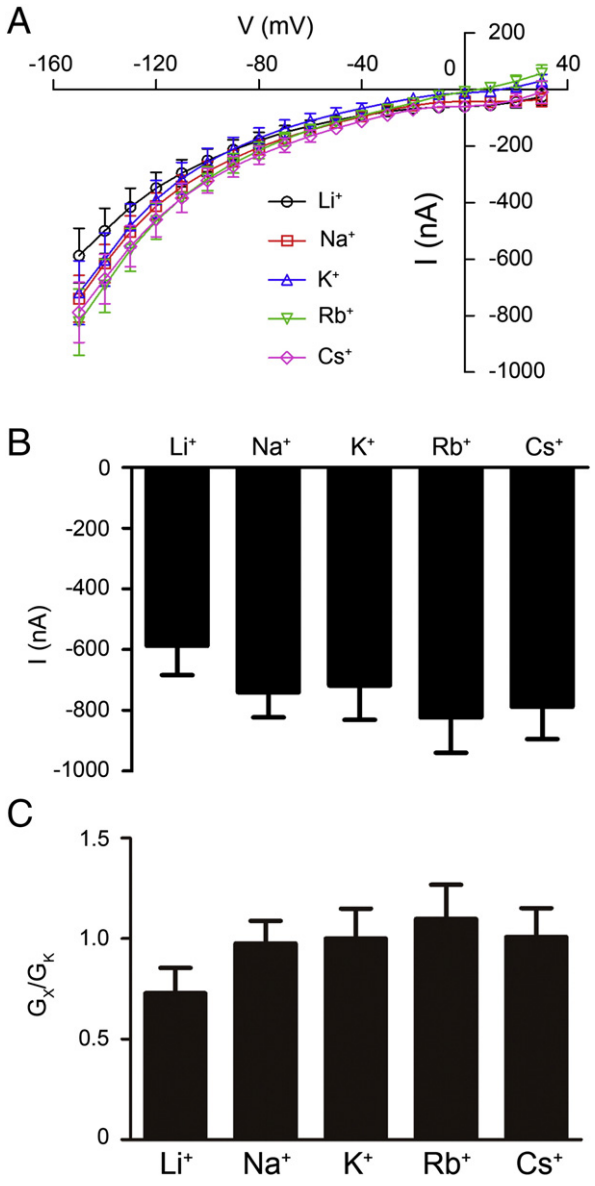

Fig. 5. Selectivity of ORF4a channel to different monovalent cations. (A) The *I/V* relationship of the currents conducted by ORF4a channel in the presence of different cations. The endogenous currents under identical conditions were subtracted. (B) Inward currents at −150 mV were recorded by TEVC with different cations in the bath solution. (C) Conductance ratio (G_X/G_K, where X represents the other cations) is the slope conductance calculated from −100 to −150 mV. Data represent the mean ± SEM (n = 6–7).

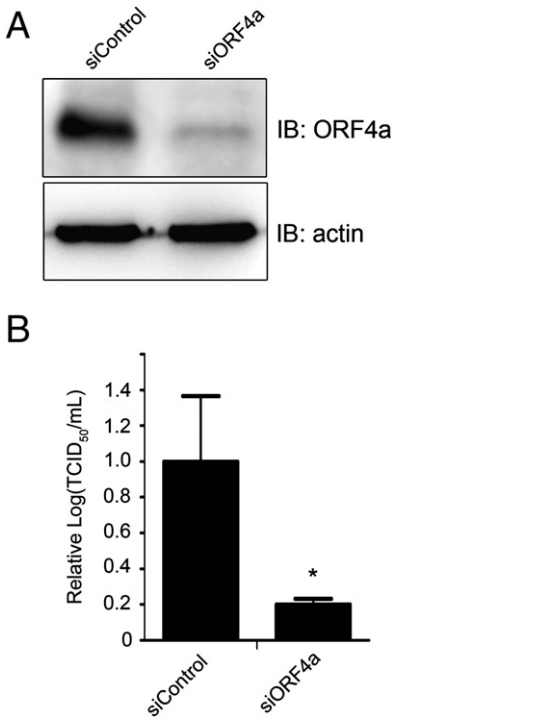

Fig. 6. The suppression of ORF4a expression inhibits virus production. (A) siRNA targeting the HCoV-229E ORF4a gene (siORF4a) or control siRNA (siControl) was transfected into Huh-7 cells before virus infection. The suppression efficiency of siORF4a was detected using a Western blot assay 48 h post-infection. (B) Supernatants containing infectious virus particles from siRNA-treated cells were titered by $TCID_{50}$ assay. Data represent the mean ± SD and were generated from three independent experiments (*$P < 0.05$, compared with siControl).

the *Paramecium bursaria* chlorella virus 1 was reported to form a potassium channel and the permeability sequence of Kcv to monovalent cations is $Rb^+ > K^+ > Cs^+ \gg Li^+ \geq Na^+$ [40,41]. The typical characteristic of ion channels is the selectivity for one type of ions [42] and this may involve in its viral life cycle regulation [43]. Considering the essential role of viroporins in the viral life cycle, channel inhibitors have become attractive drugs for an antiviral therapy [44–48]. Since the ORF4a channel showed the similar selectivity for monovalent cations to viroporins above, the inhibitors of these viroporins could have the capacity to block ORF4a channel, which should be further investigated.

The influenza A virus M2 protein is the first reported viroporin; it participates in the viral entry process by conducting protons across the viral envelope to trigger uncoating in the endosome [43,49]. HCV p7 was reported to have ion channel activity in 2003 [28,50] and shown to be crucial for efficient assembly and release of HCV particles [51]. Recently, Wozniak et al. demonstrated that intracellular H^+ conductance mediated by p7 could prevent acidification of the acidic compartments and was required for the virus production [52]. Here, we found that the number of extracellular infectious HCoV-229E particles decreased when ORF4a channel expression was suppressed by siRNA in infected cells. This demonstrates that the ORF4a protein acts as a viroporin that regulates viral production, although the details of this mechanism are unknown.

Besides their specific ion channel activity, viroporin may interact with host proteins to achieve their own ends. Vpu, a protein unique to HIV-1, is the most well studied viroporin in this field. Hsu et al. reported that Vpu induced membrane potential depolarization by interacting with a host endogenous K^+ channel TASK-1 to promote the release of viral particles [53,54]. Tetherin (also known as BST2 and CD317) is an interferon-induced transmembrane glycoprotein that tethers nascent virons on the membrane to restrict the virus release. Vpu counteracts the action of tetherin via downregulation of tetherin from the plasma membrane [55,56]. Vpu interacts with tetherin and the resulting tetherin degradation via a ubiquitin pathway was found to be relevant for this counteraction [57–59]. The SARS-CoV 3a protein has been reported to interact with caveolin-1, which is the major structural component of caveolae [60,61]. In view of the caveolae that was involved in cell cycle regulation [62] and virus uptake [63], SARS-CoV 3a was proposed to participate in these processes. Whether ORF4a protein interacts with host factors to perform functions independent of its ion channel activity need further investigation.

In summary, this study investigated the molecular properties and functions of the HCoV-229E ORF4a protein. Based on these data, we could confirm that the ORF4a protein is a viroporin that regulates virus production. This study contributes to a deeper understanding of the HCoV-229E life cycle. In addition, the identification of ORF4a as a viroporin may provide a good target for developing novel drugs against HCoV-229E.

Acknowledgements

This research was supported by grants from the National 863 project (2012AA02A404, 2012AA020103), the National Natural Science Foundation of China (31030029, 31230024 and 31100662), the National Science and Technology Major Project (2013ZX10004-101-005, 2012ZX10002-007-003), an SA-SIBS Discovery Innovation Grant and a grant from Li Kha Shing Foundation.

References

[1] P. Masters, The molecular biology of coronaviruses, Adv. Virus Res. 66 (2006) 193–292.
[2] D. Hamre, J.J. Procknow, A new virus isolated from the human respiratory tract, Proc. Soc. Exp. Biol. Med. 121 (1966) 190–193.
[3] K. McIntosh, W.B. Becker, R.M. Chanock, Growth in suckling-mouse brain of "IBV-like" viruses from patients with upper respiratory tract disease, Proc. Natl. Acad. Sci. U. S. A. 58 (1967) 2268–2273.
[4] P.A. Rota, M.S. Oberste, S.S. Monroe, W.A. Nix, R. Campagnoli, J.P. Icenogle, S. Penaranda, B. Bankamp, K. Maher, M.H. Chen, S. Tong, A. Tamin, L. Lowe, M. Frace, J.L. DeRisi, Q. Chen, D. Wang, D.D. Erdman, T.C. Peret, C. Burns, T.G. Ksiazek, P.E. Rollin, A. Sanchez, S. Liffick, B. Holloway, J. Limor, K. McCaustland, M. Olsen-Rasmussen, R. Fouchier, S. Gunther, A.D. Osterhaus, C. Drosten, M.A. Pallansch, L.J. Anderson, W.J. Bellini, Characterization of a novel coronavirus associated with severe acute respiratory syndrome, Science 300 (2003) 1394–1399.
[5] T.G. Ksiazek, D. Erdman, C.S. Goldsmith, S.R. Zaki, T. Peret, S. Emery, S. Tong, C. Urbani, J.A. Comer, W. Lim, P.E. Rollin, S.F. Dowell, A.E. Ling, C.D. Humphrey, W.J. Shieh, J. Guarner, C.D. Paddock, P. Rota, B. Fields, J. DeRisi, J.Y. Yang, N. Cox, J.M. Hughes, J.W. LeDuc, W.J. Bellini, L.J. Anderson, A novel coronavirus associated with severe acute respiratory syndrome, N. Engl. J. Med. 348 (2003) 1953–1966.
[6] J.S.M. Peiris, S.T. Lai, L.L.M. Poon, Y. Guan, L.Y.C. Yam, W. Lim, J. Nicholls, W.K.S. Yee, W.W. Yan, M.T. Cheung, V.C.C. Cheng, K.H. Chan, D.N.C. Tsang, R.W.H. Yung, T.K. Ng, K.Y. Yuen, S.S. Grp, Coronavirus as a possible cause of severe acute respiratory syndrome, Lancet 361 (2003) 1319–1325.
[7] L. van der Hoek, K. Pyrc, M.F. Jebbink, W. Vermeulen-Oost, R.J. Berkhout, K.C. Wolthers, P.M. Wertheim-van Dillen, J. Kaandorp, J. Spaargaren, B. Berkhout, Identification of a new human coronavirus, Nat. Med. 10 (2004) 368–373.
[8] P.C. Woo, S.K. Lau, C.M. Chu, K.H. Chan, H.W. Tsoi, Y. Huang, B.H. Wong, R.W. Poon, J.J. Cai, W.K. Luk, L.L. Poon, S.S. Wong, Y. Guan, J.S. Peiris, K.Y. Yuen, Characterization and complete genome sequence of a novel coronavirus, coronavirus HKU1, from patients with pneumonia, J. Virol. 79 (2005) 884–895.
[9] A.M. Zaki, S. van Boheemen, T.M. Bestebroer, A.D. Osterhaus, R.A. Fouchier, Isolation of a novel coronavirus from a man with pneumonia in Saudi Arabia, N. Engl. J. Med. 367 (2012) 1814–1820.
[10] S. van Boheemen, M. de Graaf, C. Lauber, T.M. Bestebroer, V.S. Raj, A.M. Zaki, A.D. Osterhaus, B.L. Haagmans, A.E. Gorbalenya, E.J. Snijder, R.A. Fouchier, Genomic characterization of a newly discovered coronavirus associated with acute respiratory distress syndrome in humans, MBio 3 (2012).
[11] R. Zeng, R.-F. Yang, M.-D. Shi, M.-R. Jiang, Y.-H. Xie, H.-Q. Ruan, X.-S. Jiang, L. Shi, H. Zhou, L. Zhang, Characterization of the 3a Protein of SARS-associated coronavirus in infected vero E6 cells and SARS patients, J. Mol. Biol. 341 (2004) 271–279.
[12] W. Lu, B.J. Zheng, K. Xu, W. Schwarz, L. Du, C.K. Wong, J. Chen, S. Duan, V. Deubel, B. Sun, Severe acute respiratory syndrome-associated coronavirus 3a protein forms an ion channel and modulates virus release, Proc. Natl. Acad. Sci. U. S. A. 103 (2006) 12540–12545.
[13] B. Yount, R.S. Roberts, A.C. Sims, D. Deming, M.B. Frieman, J. Sparks, M.R. Denison, N. Davis, R.S. Baric, Severe acute respiratory syndrome coronavirus group-specific open reading frames encode nonessential functions for replication in cell cultures and mice, J. Virol. 79 (2005) 14909–14922.
[14] C.-M. Chan, H. Tsoi, W.-M. Chan, S. Zhai, C.-O. Wong, X. Yao, W.-Y. Chan, S.K.-W. Tsui, H.Y.E. Chan, The ion channel activity of the SARS-coronavirus 3a protein is linked to its pro-apoptotic function, Int. J. Biochem. Cell Biol. 41 (2009) 2232–2239.
[15] M.A. Muller, L. van der Hoek, D. Voss, O. Bader, D. Lehmann, A.R. Schulz, S. Kallies, T. Suliman, B.C. Fielding, C. Drosten, M. Niedrig, Human coronavirus NL63 open reading frame 3 encodes a virion-incorporated N-glycosylated membrane protein, Virol. J. 7 (2010) 6.
[16] D.S. Song, J.S. Yang, J.S. Oh, J.H. Han, B.K. Park, Differentiation of a Vero cell adapted porcine epidemic diarrhea virus from Korean field strains by restriction fragment length polymorphism analysis of ORF 3, Vaccine 21 (2003) 1833–1842.
[17] S.J. Park, H.J. Moon, Y. Luo, H.K. Kim, E.M. Kim, J.S. Yang, D.S. Song, B.K. Kang, C.S. Lee, B.K. Park, Cloning and further sequence analysis of the ORF3 gene of wild- and attenuated-type porcine epidemic diarrhea viruses, Virus Genes 36 (2008) 95–104.
[18] K. Wang, W. Lu, J. Chen, S. Xie, H. Shi, H. Hsu, W. Yu, K. Xu, C. Bian, W.B. Fischer, W. Schwarz, L. Feng, B. Sun, PEDV ORF3 encodes an ion channel protein and regulates virus production, FEBS Lett. 586 (2012) 384–391.
[19] R.L. Nakamura, J.A. Anderson, R.F. Gaber, Determination of key structural requirements of a K+ channel pore, J. Biol. Chem. 272 (1997) 1011–1018.
[20] M.J. Adams, E.B. Carstens, Ratification vote on taxonomic proposals to the International Committee on Taxonomy of Viruses (2012), Arch. Virol. 157 (2012) 1411–1422.
[21] Y.J. Tan, E. Teng, S. Shen, T.H. Tan, P.Y. Goh, B.C. Fielding, E.E. Ooi, H.C. Tan, S.G. Lim, W. Hong, A novel severe acute respiratory syndrome coronavirus protein, U274, is transported to the cell surface and undergoes endocytosis, J. Virol. 78 (2004) 6723–6734.
[22] C.J. Yu, Y.C. Chen, C.H. Hsiao, T.C. Kuo, S.C. Chang, C.Y. Lu, W.C. Wei, C.H. Lee, L.M. Huang, M.F. Chang, H.N. Ho, F.J. Lee, Identification of a novel protein 3a from severe acute respiratory syndrome coronavirus, FEBS Lett. 565 (2004) 111–116.
[23] X. Yuan, J. Li, Y. Shan, Z. Yang, Z. Zhao, B. Chen, Z. Yao, B. Dong, S. Wang, J. Chen, Y. Cong, Subcellular localization and membrane association of SARS-CoV 3a protein, Virus Res. 109 (2005) 191–202.
[24] S. Xie, K. Wang, W. Yu, W. Lu, K. Xu, J. Wang, B. Ye, W. Schwarz, Q. Jin, B. Sun, DIDS blocks a chloride-dependent current that is mediated by the 2B protein of enterovirus 71, Cell Res. 21 (2011) 1271–1275.
[25] G. Eisenman, R. Horn, Ionic selectivity revisited: the role of kinetic and equilibrium processes in ion permeation through channels, J. Membr. Biol. 76 (1983) 197–225.
[26] W.B. Fischer, M.S. Sansom, Viral ion channels: structure and function, Biochim. Biophys. Acta 1561 (2002) 27–45.
[27] M.E. Gonzalez, L. Carrasco, Viroporins, FEBS Lett. 552 (2003) 28–34.
[28] S. Griffin, The p7 protein of hepatitis C virus forms an ion channel that is blocked by the antiviral drug, Amantadine, FEBS Lett. 535 (2003) 34–38.
[29] W.B. Fischer, J. Kruger, Viral channel-forming proteins, Int. Rev. Cell Mol. Biol. 275 (2009) 35–63.
[30] T. Suzuki, Y. Orba, Y. Okada, Y. Sunden, T. Kimura, S. Tanaka, K. Nagashima, W.W. Hall, H. Sawa, The human polyoma JC virus agnoprotein acts as a viroporin, PLoS Pathog. 6 (2010) e1000801.
[31] W.B. Fischer, H.J. Hsu, Viral channel forming proteins — modeling the target, Biochim. Biophys. Acta 1808 (2011) 561–571.
[32] J.M. Hyser, M.R. Collinson-Pautz, B. Utama, M.K. Estes, Rotavirus disrupts calcium homeostasis by NSP4 viroporin activity, MBio 1 (2010).
[33] S. Raghava, K.M. Giorda, F.B. Romano, A.P. Heuck, D.N. Hebert, The SV40 late protein VP4 is a viroporin that forms pores to disrupt membranes for viral release, PLoS Pathog. 7 (2011) e1002116.
[34] D.P. Gladue, L.G. Holinka, E. Largo, I.F. Sainz, C. Carrillo, V. O'Donnell, R. Baker-Branstetter, Z.G. Lu, X. Ambroggio, G.R. Risatti, J.L. Nieva, M.V. Borca, Classical swine fever virus p7 protein is a viroporin involved in virulence in swine, J. Virol. 86 (2012) 6778–6791.
[35] R.J. Sugrue, A.J. Hay, Structural characteristics of the M2 protein of influenza A viruses: evidence that it forms a tetrameric channel, Virology 180 (1991) 617–624.
[36] A.L. Grice, I.D. Kerr, M.S. Sansom, Ion channels formed by HIV-1 Vpu: a modelling and simulation study, FEBS Lett. 405 (1997) 299–304.
[37] G.D. Ewart, T. Sutherland, P.W. Gage, G.B. Cox, The Vpu protein of human immunodeficiency virus type 1 forms cation-selective ion channels, J. Virol. 70 (1996) 7108–7115.
[38] A. Premkumar, L. Wilson, G.D. Ewart, P.W. Gage, Cation-selective ion channels formed by p7 of hepatitis C virus are blocked by hexamethylene amiloride, FEBS Lett. 557 (2004) 99–103.
[39] T. Mehnert, A. Routh, P.J. Judge, Y.H. Lam, D. Fischer, A. Watts, W.B. Fischer, Biophysical characterization of Vpu from HIV-1 suggests a channel-pore dualism, Proteins 70 (2008) 1488–1497.
[40] B. Plugge, S. Gazzarrini, M. Nelson, R. Cerana, J.L. Van Etten, C. Derst, D. DiFrancesco, A. Moroni, G. Thiel, A potassium channel protein encoded by chlorella virus PBCV-1, Science 287 (2000) 1641–1644.
[41] S. Gazzarrini, M. Kang, A. Abenavoli, G. Romani, C. Olivari, D. Gaslini, G. Ferrara, J.L. van Etten, M. Kreim, S.M. Kast, G. Thiel, A. Moroni, Chlorella virus ATCV-1 encodes a functional potassium channel of 82 amino acids, Biochem. J. 420 (2009) 295–303.
[42] B. Roux, S. Berneche, B. Egwolf, B. Lev, S.Y. Noskov, C.N. Rowley, H. Yu, Ion selectivity in channels and transporters, J. Gen. Physiol. 137 (2011) 415–426.
[43] L.H. Pinto, L.J. Holsinger, R.A. Lamb, Influenza-virus M2 protein has ion channel activity, Cell 69 (1992) 517–528.
[44] J.L. Nieva, V. Madan, L. Carrasco, Viroporins: structure and biological functions, Nat. Rev. Microbiol. 10 (2012) 563–574.
[45] K. Wang, S. Xie, B. Sun, Viral proteins function as ion channels, Biochim. Biophys. Acta 1808 (2011) 510–515.
[46] G. Khoury, G. Ewart, C. Luscombe, M. Miller, J. Wilkinson, Antiviral efficacy of the novel compound BIT225 against HIV-1 release from human macrophages, Antimicrob. Agents Chemother. 54 (2010) 835–845.
[47] C.A. Luscombe, Z. Huang, M.G. Murray, M. Miller, J. Wilkinson, G.D. Ewart, A novel Hepatitis C virus p7 ion channel inhibitor, BIT225, inhibits bovine viral diarrhea virus in vitro and shows synergism with recombinant interferon-alpha-2b and nucleoside analogues, Antiviral Res. 86 (2010) 144–153.
[48] S. Schwarz, K. Wang, W. Yu, B. Sun, W. Schwarz, Emodin inhibits current through SARS-associated coronavirus 3a protein, Antivir. Res. 90 (2011) 64–69.
[49] A. Helenius, Unpacking the incoming influenza-virus, Cell 69 (1992) 577–578.
[50] D. Pavlovic, The hepatitis C virus p7 protein forms an ion channel that is inhibited by long-alkyl-chain iminosugar derivatives, Proc. Natl. Acad. Sci. 100 (2003) 6104–6108.
[51] E. Steinmann, F. Penin, S. Kallis, A.H. Patel, R. Bartenschlager, T. Pietschmann, Hepatitis C virus p7 protein is crucial for assembly and release of infectious virions, PLoS Pathog. 3 (2007) e103.
[52] A.L. Wozniak, S. Griffin, D. Rowlands, M. Harris, M. Yi, S.M. Lemon, S.A. Weinman, Intracellular proton conductance of the hepatitis C virus p7 protein and its contribution to infectious virus production, PLoS Pathog. 6 (2010) e1001087.
[53] K. Hsu, J. Seharaseyon, P.H. Dong, S. Bour, E. Marban, Mutual functional destruction of HIV-1 Vpu and host TASK-1 channel, Mol. Cell 14 (2004) 259–267.
[54] K. Hsu, J. Han, K. Shinlapawittayatorn, I. Deschenes, E. Marbán, Membrane potential depolarization as a triggering mechanism for Vpu-mediated HIV-1 release, Biophys. J. 99 (2010) 1718–1725.
[55] S.J.D. Neil, V. Sandrin, W.I. Sundquist, P.D. Bieniasz, An interferon-alpha-induced tethering mechanism inhibits HIV-1 and Ebola virus particle release but is counteracted by the HIV-1 Vpu protein, Cell Host Microbe. 2 (2007) 193–203.
[56] N. Van Damme, D. Goff, C. Katsura, R.L. Jorgenson, R. Mitchell, M.C. Johnson, E.B. Stephens, J. Guatelli, The interferon-induced protein BST-2 restricts HIV-1 release

and is downregulated from the cell surface by the viral Vpu protein, Cell Host Microbe. 3 (2008) 245–252.
[57] J.L. Douglas, K. Viswanathan, M.N. McCarroll, J.K. Gustin, K. Fruh, A.V. Moses, Vpu directs the degradation of the human immunodeficiency virus restriction factor BST-2/tetherin via a beta TrCP-dependent mechanism, J. Virol. 83 (2009) 7931–7947.
[58] B. Mangeat, G. Gers-Huber, M. Lehmann, M. Zufferey, J. Luban, V. Piguet, HIV-1 Vpu neutralizes the antiviral factor tetherin/BST-2 by binding it and directing its beta-TrCP2-dependent degradation, PLoS Pathog. 5 (2009).
[59] R.S. Mitchell, C. Katsura, M.A. Skasko, K. Fitzpatrick, D. Lau, A. Ruiz, E.B. Stephens, F. Margottin-Goguet, R. Benarous, J.C. Guatelli, Vpu antagonizes BST-2-mediated restriction of HIV-1 release via beta-TrCP and endo-lysosomal trafficking, PLoS Pathog. 5 (2009).
[60] Q.C. Cai, Q.W. Jiang, G.M. Zhao, Q. Guo, G.W. Cao, T. Chen, Putative caveolin-binding sites in SARS-CoV proteins, Acta Pharmacol. Sin. 24 (2003) 1051–1059.
[61] K. Padhan, C. Tanwar, A. Hussain, P.Y. Hui, M.Y. Lee, C.Y. Cheung, J.S. Peiris, S. Jameel, Severe acute respiratory syndrome coronavirus Orf3a protein interacts with caveolin, J. Gen. Virol. 88 (2007) 3067–3077.
[62] J. Hulit, T. Bash, M.F. Fu, F. Galbiati, C. Albanese, D.R. Sage, A. Schlegel, J. Zhurinsky, M. Shtutman, A. Ben-Ze'ev, M.P. Lisanti, R.G. Pestell, The cyclin D1 gene is transcriptionally repressed by caveolin-1, J. Biol. Chem. 275 (2000) 21203–21209.
[63] L. Pelkmans, J. Kartenbeck, A. Helenius, Caveolar endocytosis of simian virus 40 reveals a new two-step vesicular-transport pathway to the ER, Nat. Cell Biol. 3 (2001) 473–483.